Case Study: Detection of Turn-to-Turn Faults in a Load Tap Changer Mechanism

Craig Cosgrove
MATEP LLC.

Austin Burfield and Zachary Summerford
Schweitzer Engineering Laboratories, Inc.

Presented at the
79th Annual Conference for Protective Relay Engineers
College Station, Texas
March 30–April 2, 2026

Case Study: Detection of Turn-to-Turn Faults in a Load Tap Changer Mechanism

Craig Cosgrove, *MATEP LLC.*
Austin Burfield and Zachary Summerford, *Schweitzer Engineering Laboratories, Inc.*

***Abstract*—A 138 kV/13.8 kV/13.8 kV delta-wye-wye distribution transformer experienced a turn-to-turn fault in the load tap changer (LTC) tank. This fault evolved to involve multiple tap leads feeding the same phase at the bulkhead of the LTC, effectively creating a turn-to-turn fault. While the phase differential relay, set with typical values based upon the base megavolt-ampere rating, operated correctly for the fault, further investigation of the oil and subsequent damage revealed that the fault had likely been present for some time. Analysis of the LTC shoes and contacts indicated that the cause of the fault is believed to have been the result of inadequate contact within the mechanism, which led to an increase in heat and insulation breakdown. Turn-to-turn faults are known to challenge phase differential element sensitivity. Event analysis shows that the initial fault was below the minimum sensitivity of the phase differential element until evolution of the fault led to an increase in current magnitude, allowing the protective relay to operate.**

This paper provides analysis of the operation and performance of the existing restrained and unrestrained phase differential protection elements. In addition, the paper presents an analysis of the recorded fault data before the relay operation to show how a protection element, such as a negative-sequence current differential element, can supplement the phase differential protection for increased sensitivity for low-grade faults that may otherwise go undetected and result in significant equipment damage.

I. Introduction

Turn-to-turn faults are a source of frustration for equipment engineers and protection engineers alike. Traditional protection methodologies rely on mechanical or gas spectrometer analysis to determine the presence of an anomaly that has already developed into a fault, or one that may be an indication of a pending failure. The operation we present in this paper highlights an example where traditional protection operated correctly to clear a fault after it transitioned from a turn-to-turn fault to a fault involving multiple taps within the load tap changer (LTC). In this paper, we highlight the use of a negative-sequence differential element for the detection of turn-to-turn faults that may go undetected by traditional phase differential protection.

In Section II, we provide an overview of the system under study and the connection of the power transformer that is discussed in the operation. In Section III, we describe in more detail the nature of the fault (as it was detected by the phase differential element), the damage observed, and the event data recorded. In Section IV, we provide a brief refresher on the principles of phase differential protection as it pertains to power transformers and potential sensitivity limitations. In Section IV, we introduce the negative-sequence differential element and highlight the increase in sensitivity and the improvements in coverage obtained by using the event data captured during a known turn-to-turn fault. In Section V, we compare the sensitivity and coverage of the traditional phase differential element with the addition of the negative-sequence differential element.

II. System and Transformer Overview

The subject system consists of a 135.5 kV ring bus feeding three 45/60/75 megavolt-ampere (MVA) transformers. Each of the transformer voltage ratings and winding connections are as follows:

HV: 134.5 kV, delta connected
LV1: 13.8 kV, wye-grounded
LV2: 13.8 kV, wye-grounded

The secondary windings are connected to a networked ring bus through circuit breakers. Fig. 1 shows a portion of the system in question.

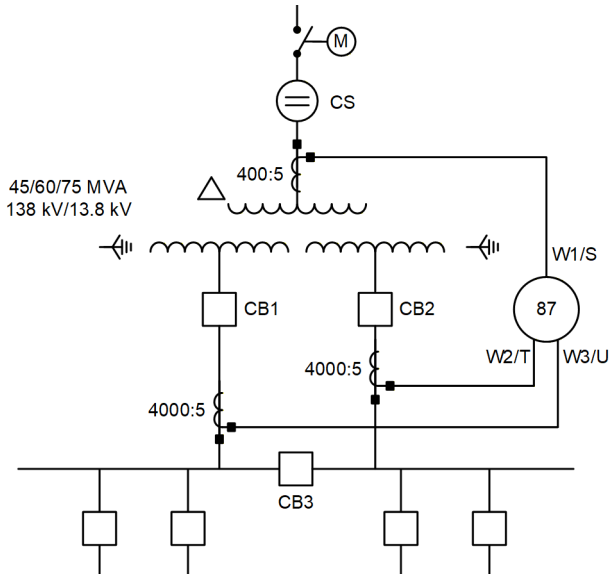

Fig. 1 System One-Line Diagram

The transformers are equipped with arc-in-oil-type on-load tap changers (OLTCs) on both secondary windings. Transformer protection is provided by directional overcurrent relays on the primary circuit switches of the transformer and phase current differential relays for complete transformer isolation via the circuit switches and 13.8 kV secondary breakers. The transformer main tank and OLTC tanks are equipped with

pressure relief devices, though only the main tank is equipped with a sudden pressure relay.

III. Event Description

In the late summer of 2024, a prominent midwestern university electrical department was notified by operations that there had been a trip in one of the main substations. Upon arrival and further inspection by substation technicians, it was observed that oil had been discharged around the X winding of one of the transformers. Upon further investigation, requiring the draining of oil from both the OLTC tank and transformer main tank, technicians discovered that the transformer had suffered a severe turn-to-turn fault in the X3 cabling of the respective OLTC. The fault caused the isolation of the affected transformer via the transformer differential relay on C-phase.

A post-fault physical analysis concluded that the likely root cause of the fault was the failure between the moving and stationary selector contacts within the OLTC. Fig. 2 shows the configuration of the type of OLTC that was in operation at the time of this event. The OLTC, as shown in Fig. 2, is in the 16L tap position with both moving selector contacts G and H located on the Number 4 stationary contact. While the reversing switch is connected to R and A, the turns between tap Number 4 and Number 12 are connected between Number 2 and Number 14 of the overall transformer winding in a subtractive polarity, thus reducing the overall effective ratio. This type of OLTC uses reactive switching with a preventative autotransformer when transitioning from one tap position to another. When transitioning from one tap position to the next, the Transfer Switches E and F, and the Preventative Autotransformer, P1, P2, and P3, are used to prevent arcing across the moving and stationary selector contacts. The arcing that occurs when the current is interrupted temporarily in the reactor loop takes place within an arc chute and should not occur at the selector switch contacts.

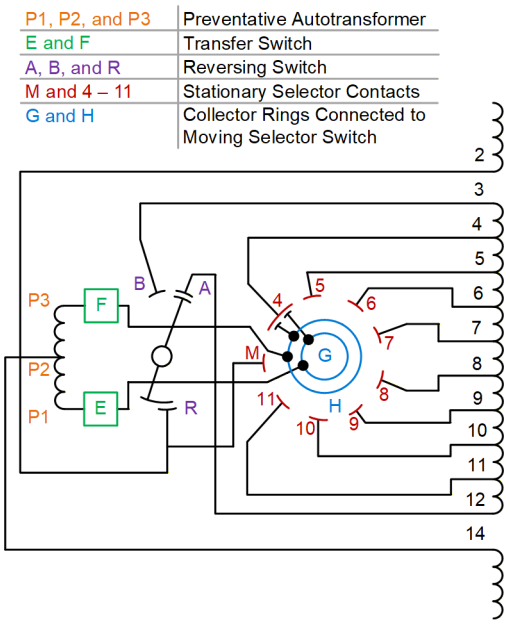

Fig. 2 OLTC Diagram

Fig. 3 and Fig. 4 show the damage to the stationary selector contact of the OLTC and the subsequent cable failure, respectively. The contact failure resulted in the OLTC oil being carbonized and significant gassing, which caused rapid dielectric breakdown of the oil and generation of heat which caused breakdown of the insulation of the cables. The combined loss of dielectric led to cable failure resulting in a turn-to-turn fault. This turn-to-turn fault is not traditional in the sense that it involves a single turn of the winding but rather across two cables that represent up to 10 percent or more of the winding feeding the taps of the OLTC.

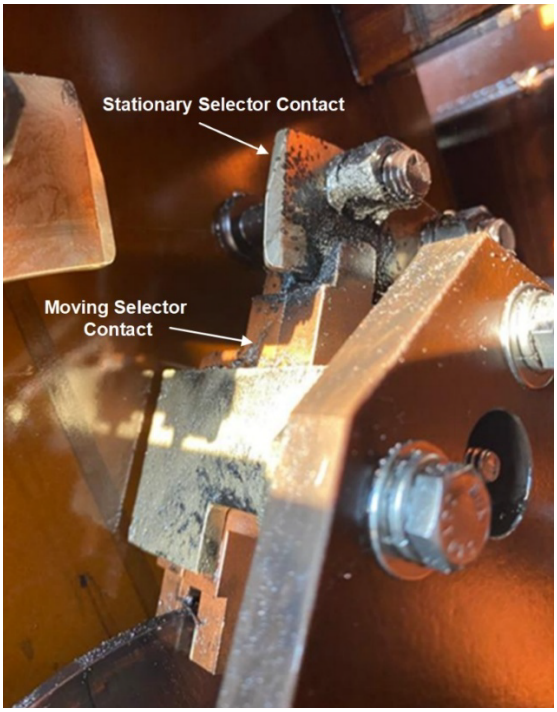

Fig. 3 Selector Switch Damage Within OLTC

Fig. 4 Cable Failure at OLTC Tap Board on Bulkhead

The fault caused significant damage to the OLTC, the cabling, and the tap bulkhead. This bulkhead, which covers and seals the cable passage between the main transformer tank and the OLTC tank, did prevent damage inside the main tank. The bulkhead being damaged was significant in its effect on the transformer repair, because replacing it required draining and entering the main tank, which would not have been required otherwise.

IV. Differential Protection Overview

Transformer protection, as described in [1] and [2], often relies on a phase differential element as one of the primary methods of detecting faults within the zone of protection. In principle, differential elements rely on Kirchoff's current law (KCL), which states that the sum of currents entering a node must equal the sum of currents leaving a node. For equipment such as buses, rotating machines, and lines, this principle works out nicely, but one must consider the presence of standing differential, because of unequal CT performance and unmetered loads within the zone of protection. However, when differential protection is applied to transformers, one must now consider the ampere-turn balance (ATB) and understand where there may exist additional sources of standing differential current, such as transformer excitation current. To account for the presence of standing differential current in either a KCL- or ATB-based scheme, a percentage restrained differential device is often used where the measured operating current within the zone of protection must exceed a specified percentage of the restraining current that represents the total current flowing through the zone of protection.

Fig. 1 shows the protection one-line diagram of a delta-wye-wye transformer being protected by a phase differential relay. One of the main benefits of using a differential relay is that the minimum sensitivity of the device does not depend on load flow, system unbalances, or faults external to the zone of protection.

Protection of a transformer often requires compensation of the phase shift when a delta winding is present as well as accommodating the difference in zero-sequence current that may or may not flow on either side of the transformer. Traditional protection using electromechanical relays required creative wiring of the CTs secondary windings before they are brought into the differential relay. Modern microprocessor relays allow for compensation to be handled mathematically.

The transformer described in Section II is constructed as a DABy or Dyn1, where the polarity side of the H1 winding is connected to the non-polarity side of the H2 winding, and so on. With traditional phase-to-bushing connections of A to H1, B to H2, C to H3, and likewise for the secondary windings and a system phase rotation of ABC, the high voltage leads the low voltage by 30°. To properly compensate for the phase shift, the wye-connected windings need to have the same "delta" phase shift applied. When using external compensation, the current transformers on the wye winding would be connected in the same DAB connection. This external connection has the benefit of accommodating the phase shift but also acts to remove the zero-sequence current seen from the grounded neutral of the wye winding. Microprocessor relays allow for a wye connection in the CTs, and account for the phase shift and zero-sequence removal mathematically [3][4].

One common manufacturer of microprocessor relays uses a set of compensation matrices to achieve the desired 30° phase shift and zero-sequence removal. Table I**,** in Appendix A, shows a list of the available matrices and their resulting phase shifts. The relay described in this paper used a compensation matrix of one for both wye windings. The delta winding of the power transformer traps zero-sequence current natively; therefore, no additional phase shift or compensation is required and a compensation matrix of zero is used for the delta winding.

To properly calculate an operate and restraint current, the relay must use the compensated currents from the wye winding as given by (1), (2), and (3).

$$IAmC = \frac{(IAm - IBm)}{\sqrt{3}} \tag{1}$$

$$IBmC = \frac{(IBm - ICm)}{\sqrt{3}} \tag{2}$$

$$ICmC = \frac{(ICm - IAm)}{\sqrt{3}} \tag{3}$$

where:

m is the winding designation (i.e., S, T, and U)

Once the compensated currents have been calculated by the relay and normalized per each winding TAP, a common calculation for the operate (I_{OP}) and restraint (I_{RT}) are given by (4) and (5).

$$I_{OPn} = |\overline{InSC} + \overline{InTC} + \overline{InUC}| \tag{4}$$

$$I_{RTn} = |\overline{InSC}| + |\overline{InTC}| + |\overline{InUC}| \tag{5}$$

where:

n = A, B, and C

When analyzing the events from a transformer differential, a key take away is that the operate and restraint quantities contain contributions from multiple phases due to the compensation required to accommodate phase shift and zero-sequence removal. For example, the A-phase differential zone, 87R1, contains contributions from A-phase and B-phase currents due to the compensation matrix applied to the wye windings. The B-phase and C-phase differential zones, 87R2 and 87R3 respectively, contain similar combinations of current.

Partial winding faults, however, offer one major challenge for traditional phase differential protection. The shorting of a small percentage of turns within a single winding results in a significant amount of localized current within the shorted turns, but due to the autotransformer effect, might not produce a significant current at the terminals of the zone of protection. Partial winding faults do not often depress the voltage enough to eliminate the outfeed, which, in addition to the load on the transformer, adds to the restraint current through the zone, thus impacting the sensitivity of the phase differential element in detecting partial winding faults. Partial winding faults that involve a small number of turns may go undetected by phase differential elements until the damage is severe enough to increase the number of turns involved, resulting in larger portions of the equipment requiring repair or replacement.

A negative-sequence differential element can improve relay sensitivity for partial winding faults providing a comprehensive protection scheme for critical power transformers. During balanced system conditions, the negative-sequence element is unaffected by changes in load, thus the element can maintain a great deal of sensitivity under varying system loading [5][6].

As an example, one modern microprocessor relay uses the filtered compensated currents as determined by (1), (2), and (3)

to calculate the negative-sequence current per windings, as shown in (6).

$$3I2mC = [1 \quad \alpha^2 \quad \alpha] \bullet \begin{bmatrix} IAmC \\ IBmC \\ ICmC \end{bmatrix} \tag{6}$$

where:

m is the winding designation (i.e., S, T, and U)

α is a unit vector of $1 \angle 120°$

α^2 is a unit vector of $1 \angle 240°$

From the calculated negative-sequence currents for each winding, the relay can then calculate a resulting operate and restraint current. An example calculation is given in (7) and (8).

$$IOP87Q = \left|\sum 3I2mC\right| \tag{7}$$

$$IRT87Q = max(|3I2mC|) \tag{8}$$

where:

m is the winding designation (i.e., S, T, and U)

By using the maximum of the calculated negative-sequence currents, the restraining quantity is not as high as what was calculated in (5), resulting in additional sensitivity.

V. Comparison of Phase Differential and Negative-Sequence Differential Performance.

A. Sensitivity Concerns for This Application

When reviewing the application of differential protection to this specific transformer, the typical sources of error are easily recognized. Transformer magnetizing current and losses, CT error, and relay error all contribute to false differential values and should always be considered when selecting appropriate settings for a transformer differential [7]. The inclusion of an LTC on both the X and Y windings also introduces a source of differential error. These LTCs are dynamic and must be considered by increasing minimum pickup and slope sensitivity. For two-winding transformers, this is typically done by adding the maximum tap percent to the other calculated error sources. The three windings of this transformer do not have the same MVA ratings, the high-side +65°C (149°F) rating is 84 MVA for the H winding and 42 MVA each for the X and Y windings. Because each of the low-side windings are rated at half of the maximum transformer full-load amperes (FLA), the maximum error contribution to the differential is half of the maximum tap percent per winding. Equation (9) shows an error calculation of the two tap changers using the nameplate data of 0.5 pu of power rating and ±10 percent, or 0.1 pu for the LTC.

$$0.5\,pu \bullet 0.1\,pu + 0.5\,pu \bullet 0.1\,pu = 0.1\,pu \tag{9}$$

While the result is the same as for a two-winding transformer with a single low-side OLTC, this calculation illustrates how both low-side windings must be considered when calculating the OLTC error. For in-service settings, the relay engineer selected the +65°C (149°F) rating of 84 MVA for their calculations.

In this case study, the transformer has additional challenges that may lead to common settings mistakes. A high-side no-load tap changer that can be set ±5 percent must be accurately described in the relay settings for correct tap calculation. The H-winding no-load tap changer is static and can be compensated directly in the relay tap calculation by using the selected voltage tap as the nominal voltage for the winding. For the differential to balance properly, the tap calculations for the X and Y windings must be done on the higher H winding MVA base, meaning that when the transformer is running at FLA, each of these windings produces compensated phase currents for the differential element with a magnitude of 0.5 pu.

Overall, using common methodologies, a total slope setting for the phase differential can be calculated using factors described by the relay manufacturer. This can typically be found in the instruction manuals for the device being placed in service.

B. Review of Phase Differential Element Settings

In this application, a common microprocessor-based transformer protective relay was applied using methods typical to the industry and this application. All CTs were connected to the relay in a wye configuration. Tap values were auto calculated by the relay. The settings the relay used for the dual-slope percentage-restrained phase differential element are shown in Appendix B.

C. Plotting Percent-Restrained Differential Elements

Percentage-restrained differential elements can be visualized in one of two common ways. The first is to plot the data set along a time axis with IOP being compared to the static threshold of O87P, while the ratio of IOP/IRT is compared to a static threshold of SLP1. If a fixed dual-slope characteristic is used, IRT can be compared to an inflection point, IRS1, where the slope of the characteristic increases from SLP1 to SLP2. To assert the differential element, the ratio of IOP/IRT must be greater than the representations of the compound slope line, while IOP is also greater than O87P. While this representation is easily produced in common event analysis software, it can be difficult to intuitively interpret the data provided from a time-based event recording.

A second method for plotting these elements is to use a tool such as Mathcad to create the IOP and IRT plane and plot each of the protection element settings as straight lines, then plot the event data as a locus in this plane. Our analysis also uses this method as an additional means to illustrate the performance of each protection element for clarity.

D. Performance Evaluation of Phase Differential Element

The in-service relay recorded event data triggered by the operation of the 87R element. Raw data are recorded that includes the digital samples of the analog phase currents with minimal processing. Filtered data were also recorded that used cosine or other filters based on relay type to preserve only the fundamental frequency and harmonic frequency components of the raw sampled signals. Filtered data are most commonly used in the calculation of inputs for protection elements. Three event files, a 32 sample-per-cycle raw event containing phase currents, a filtered 4-sample-per-cycle event containing phase currents, and a raw 4-sample-per-cycle event containing differential operating quantities were retrieved by substation technicians.

Examining the raw data for the phase currents, all phases and windings appear to be irregular. C-phase on Winding 2, which was faulted, has significant deviation from its pre-fault pattern at around the –40 ms mark, as shown in Fig. 5.

Harmonic analysis of these currents indicates that C-phase was as high at 16.68 percent total harmonic distortion with the 2nd harmonic content greater than 10 percent when compared to the fundamental, 60 Hz, component. It was assumed at this point that additional damage occurred inside the LTC tank.

Examination of the recorded differential data shows that prior to this change IOP3 was around 0.2 pu below the minimum threshold of O87P. When the change in currents occurred, IOP3 did increase to as much as 0.4 pu; however, a simultaneous increase in second harmonic content triggered second harmonic blocking, delaying the element by 2 cycles. The differential element quantities are illustrated in Fig. 6.

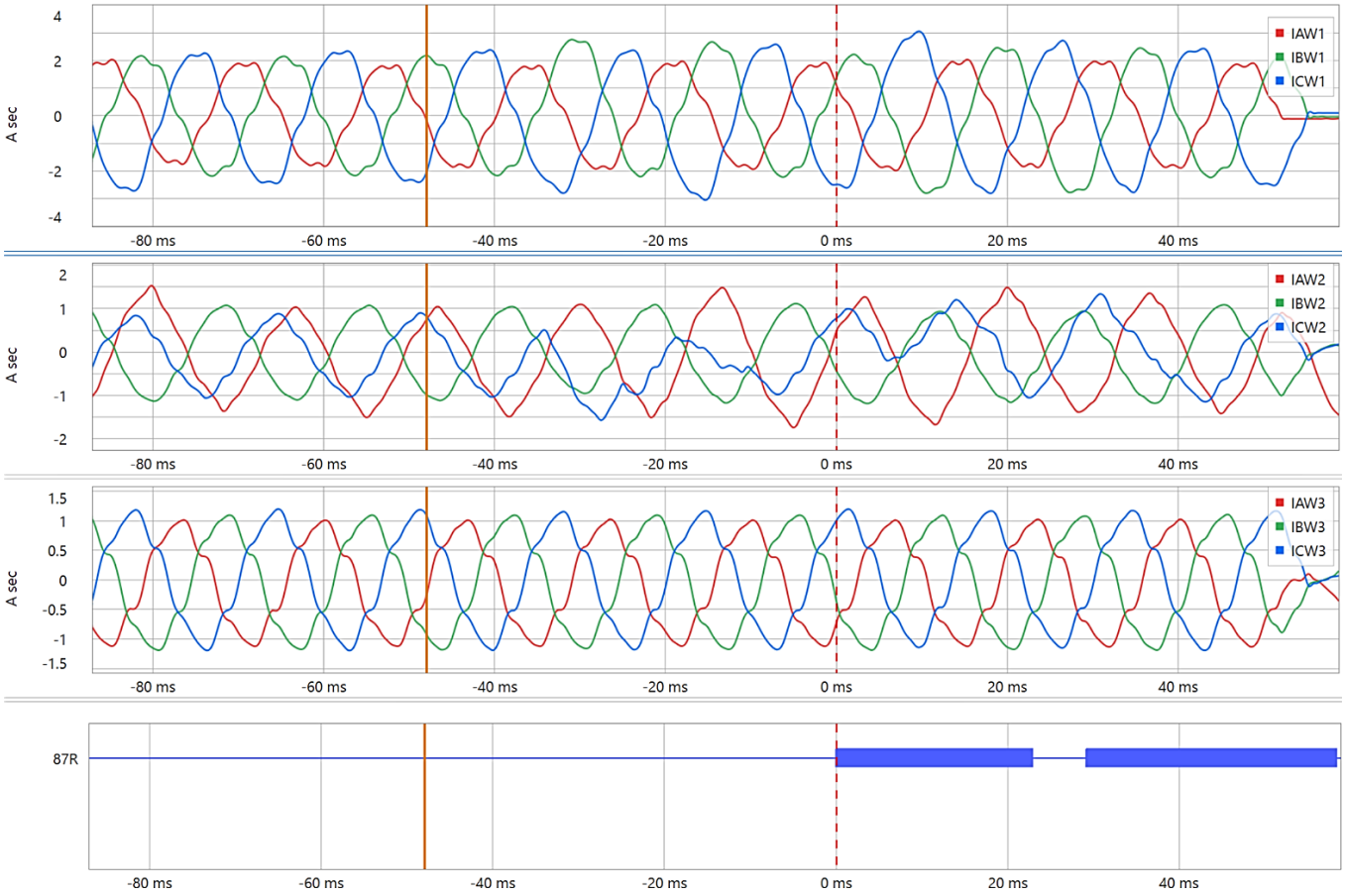

Fig. 5 Raw Phase Currents Recorded by Relay in Service

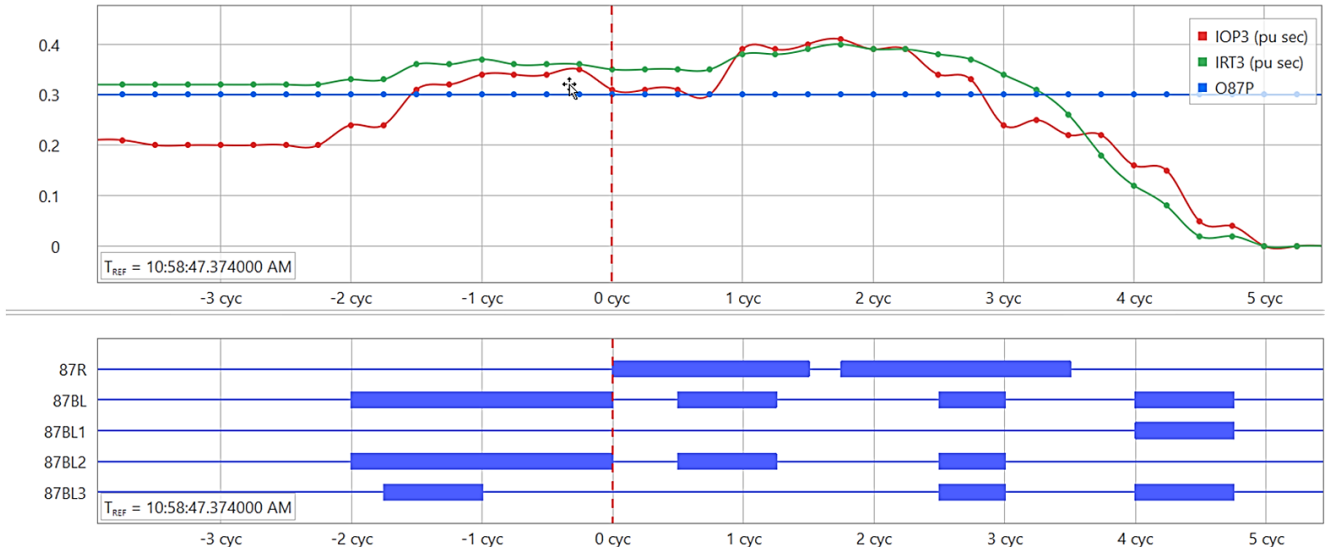

Fig. 6 87R3 IOP, IRT, and Element and Blocking Digitals

Plotting the locus of all three 87R phase differential elements, reveals that elements 87R1 and 87R2 never exceeded the minimum pickup threshold and only 87R3 operated. Fig. 7 illustrates all three elements in the IOP and IRT plane with the plot limited to 0.5 pu on each axis.

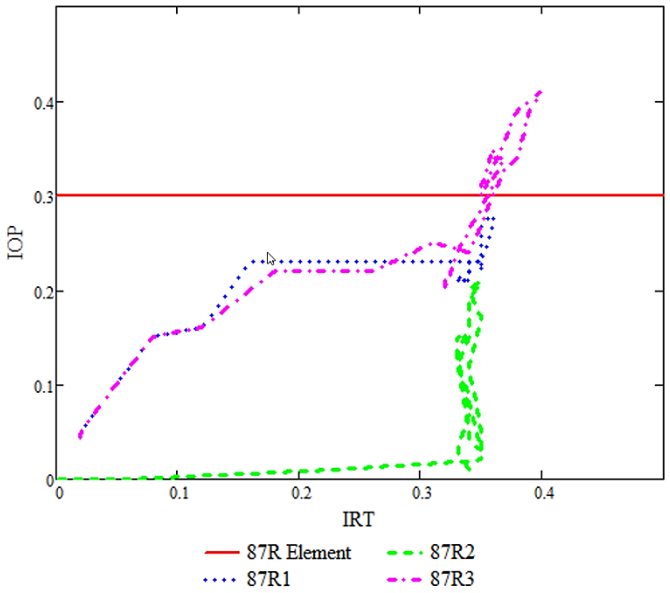

Fig. 7 Recorded Data Restrained Phase Differential Locus

To evaluate the sensitivity of the phase differential element to turn-to-turn faults such as this, the scales of the two axes were increased to include the entire operating characteristic. By increasing the scales, it can be observed in Fig. 8, that the recorded differential plots are in a low-magnitude area of the characteristic. This illustrates how this particular fault challenged 87R sensitivity.

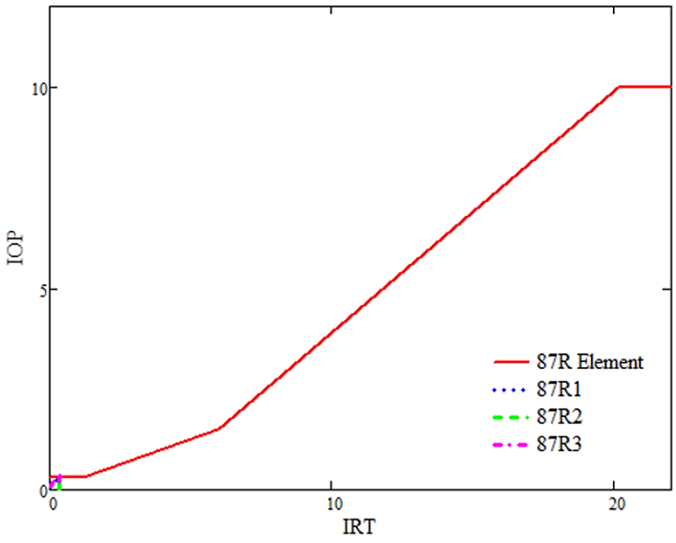

Fig. 8 Expanded View of Fig. 7

While the 87R3 element did ultimately operate and trip the transformer out of service, it appears there were indications the fault had occurred prior to this event recording. Because of the sensitivity challenges, which are due to the nature of turn-to-turn faults, and the reduction in per unit currents produced, because of the unequal winding power ratings, the phase differential element only operated after the fault evolved to the point where there was a differential greater than 0.3 pu of the transformer capacity.

E. Review of Default Negative-Sequence Differential Element Settings

A different model of microprocessor-based relay, from the same manufacturer, was selected to compare to the phase differential element performance of the in-service relay. Unlike the in-service relay, this relay is equipped with a negative-sequence current-based adaptive-slope differential element. All nameplate settings were set to the same values for both relays and the default negative-sequence differential settings values were used apart from the differential time delay, 87QD. The delay setting was selected to be 2 cycles, the minimum setting because of the limited pre-trip data that were available in the event records from the in-service relay. CT ratios, transformer ratings, nominal voltages, and tap settings applied are the same as the in-service relay. New settings were applied as shown in the following:

Enable 87Q Element: E87Q = Y

Negative-Sequence 87 Element Pickup: 87QP = 0.30

Negative-Sequence 87 Element Slope: SLPQ1 = 25 percent

Negative-Sequence 87 Element Delay: 87QD = 2 cycles

F. Method of Simulating Negative-Sequence Differential Element

Using common event analysis software, the negative-sequence differential element available in the second model of relay was recreated using custom calculations and applied to the data recorded by the in-service relay. This implementation used both custom analog quantities and custom digital quantities to fully implement the negative-sequence element. The custom calculations used to create this element are shown in Appendix C.

To aid in visual representation of the data set, the protective element was also implemented using Mathcad. This method uses the first 8 cycles of raw data recorded by the in-service relay. The first 8 cycles were selected to eliminate zero-current data after the in-service breaker tripped.

In addition, the data from the in-service relay were replayed using a secondary current injection test set into the second model of relay to validate the performance of the 87Q element. The data from the in-service relay were modified into a format that was able to be replayed as a COMTRADE file through the secondary injection test set. Metering checks and a comparison of original raw data recordings to the replayed data recordings were completed to ensure the data were replayed correctly into the second relay.

G. Performance Evaluation of Negative-Sequence Differential Element

By applying the calculations from Section F above to the 4-sample-per-cycle filtered data recorded by the in-service relay to create the negative-sequence differential element, analog and digital values associated with the custom calculations can be visualized on a time axis. By plotting

IOP87Q, IRT87Q, and the element minimum pickup, 87QP, it can be seen in Fig. 9 that IOP87 was greater than 87QP for the first 8 cycles except for one data point at –1.75 cycles and again after the breaker had tripped. Plotting the calculated slope of IOP87Q and IRT87Q against the SLPQ setting of 25 percent, we see, in Fig. 9, that the slope was greater than 160 percent through the first 8 cycles of recorded data. Plotting the custom 87QPOUT digital in Fig. 9 shows that while there is a brief dropout at t = –1.75 cycles due to a decrease in IOP87Q, the 87Q element is asserted throughout the first 8 cycles.

Using Mathcad, the same data can be used to plot the operating characteristic and the operate and restraint quantities at each sample on the IOP and IRT plane. The locus of the data in Fig. 10 shows, similarly to the time plots in Fig. 9 the element was in the operate region for the entirety of the first 8 cycles of data with two exceptions.

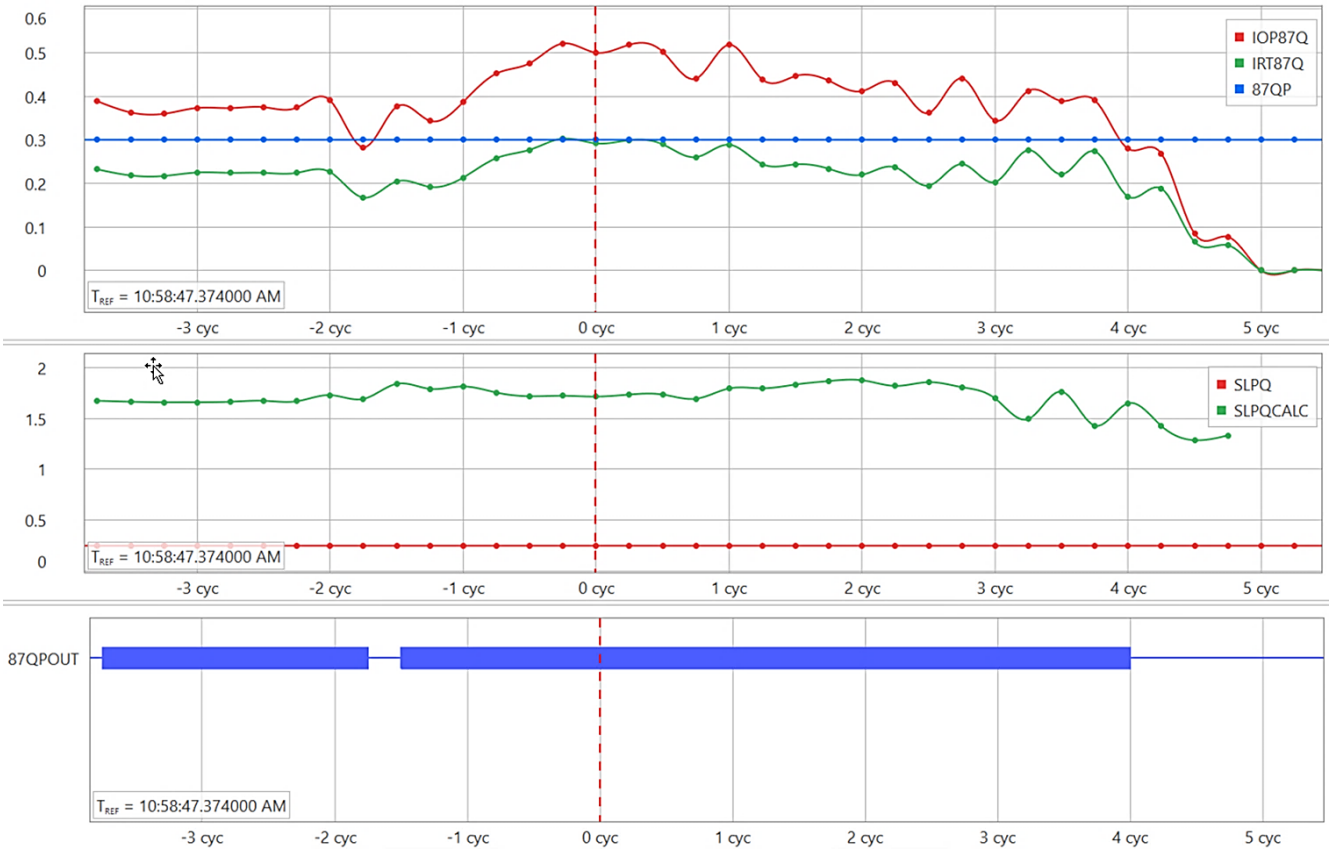

Fig. 9 Simulated 87Q Using Custom Calculations

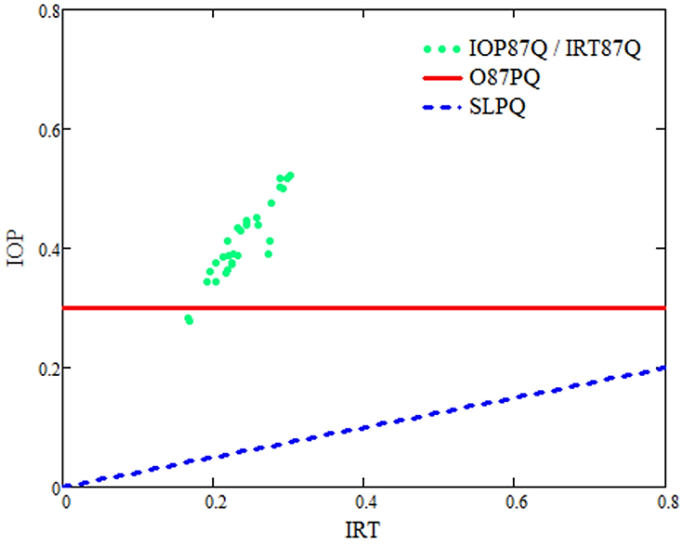

Fig. 10 Locus of Simulated 87Q Element Using Raw Data Recording

A third, more realistic evaluation of the 87Q element performance can be achieved through the replay of the event data into a model of relay that has the 87Q element available. This device recorded a compressed filtered event file at 8 samples/cycles that includes all phase and differential analogs and digitals in one file. The event playback does not include artificial pre-fault load, so the event recording begins with zero current on all channels. Plotting the recorded analog values of IOP87Q and IRT87Q in Fig. 11 shows that by allowing for a data processing rate of the test relay, which is double that of the filtered data from the in-service relay, the waveforms are nearly identical, validating the mathematical models employed. The device used for playback testing uses a one-cycle cosine filter on all currents, but the digital element 87PQ, the pickup of the negative-sequence differential, asserts within 3/4 cycles of the first non-zero data injected into the relay. The 87Q bit (the time delayed output of the 87Q) then asserts and issues TRPXFMR 2 cycles later, as seen in Fig. 11.

While the maximum magnitude of IOP87Q was still small, the data provided indicates that the 87Q element would have operated prior to 87R.

While this discussion is aimed at showcasing the sensitivity of the negative-sequence differential element, there is considerable concern within the industry surrounding the security of the element for external system conditions. Fig. 12 shows a simulation of the transformer described in Section I with only one secondary winding loaded to 1 pu and roughly 10 percent of FLA negative-sequence current flowing through the zone. As can be seen in the third axis of the plot, the resulting IOP87Q is 0.007 pu with 10 percent of negative-sequence current flowing through the transformer. The calculated restraint, IRT87Q, is 0.281 pu, which results in a mismatch of approximately 2.5 percent.

To gain security during external faults and events causing CT saturation, the use of an external fault detector or CT saturation detection algorithms can be used to add delay or block the 87Q element to prevent misoperation [3].

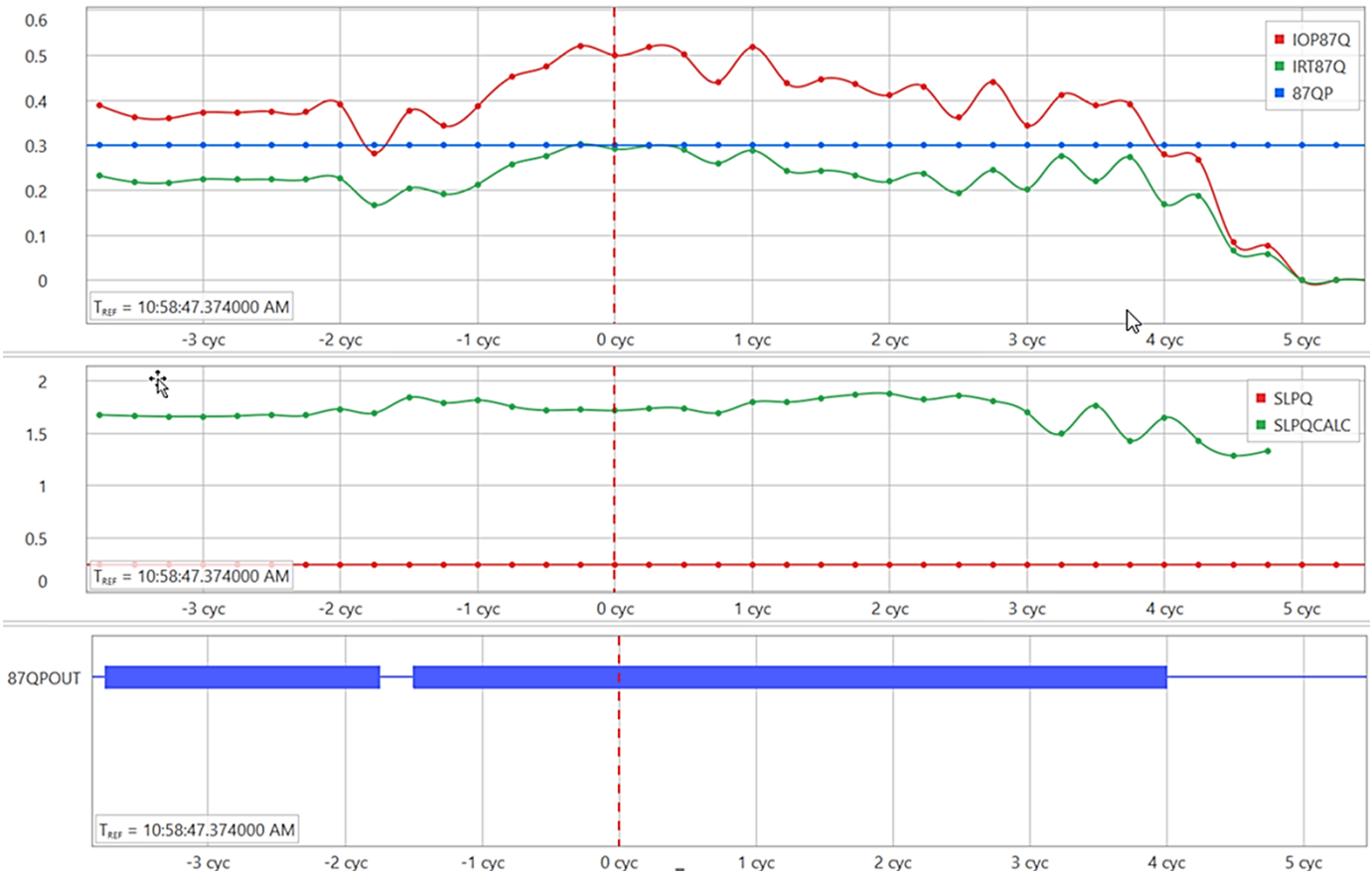

Fig. 11 Playback Record From Relay With 87Q Enabled

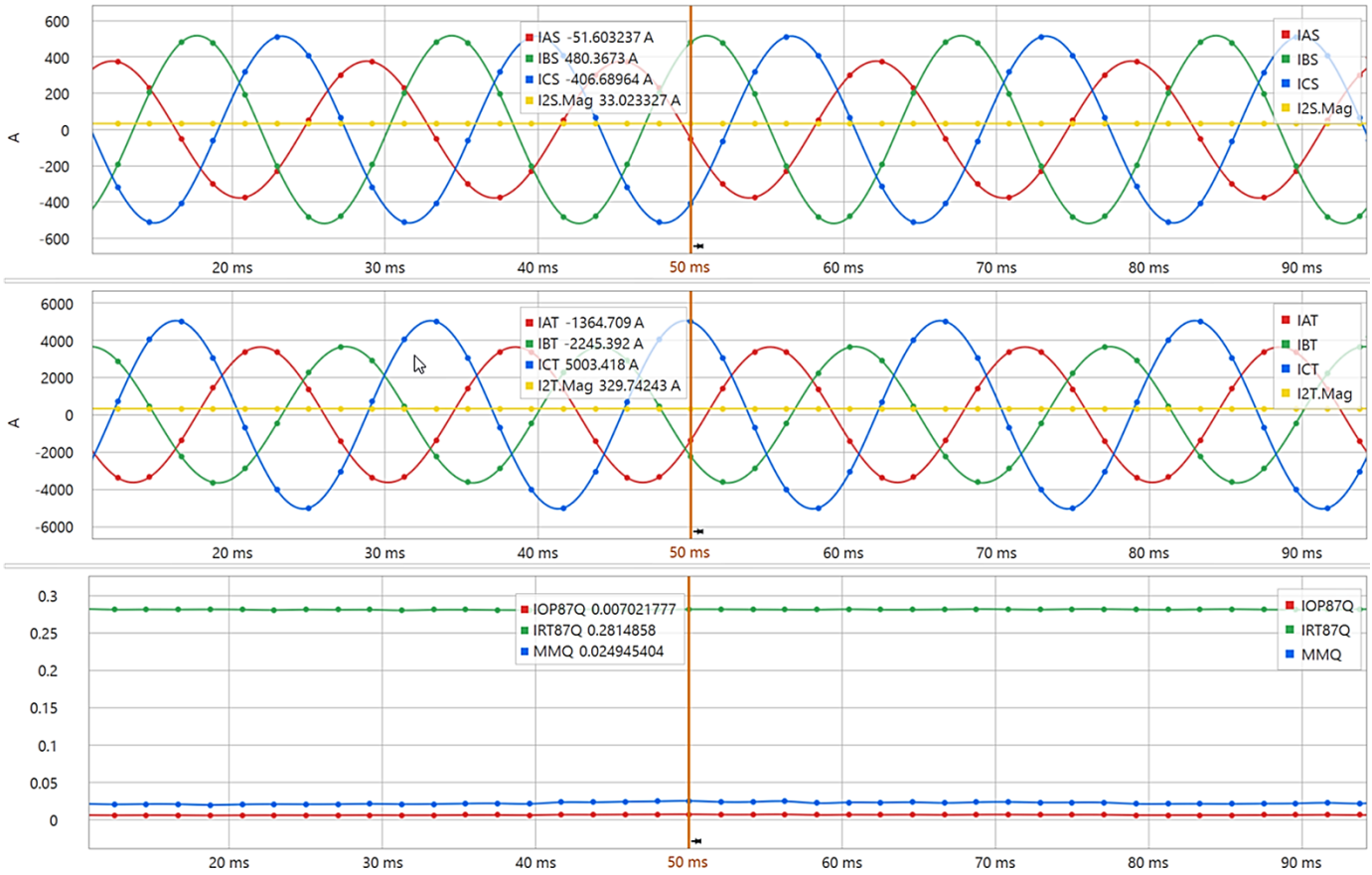

Fig. 12 Simulation of 10 Percent Load Unbalance

H. Comparison of Phase and Negative-Sequence Differential Element Performance

There are several factors in this particular case that challenge the sensitivity of the phase differential element. First, the unequal power ratings of the three windings create lower IOP contributions from the secondary windings than would be seen in a two-winding transformer. In addition, the nature of a turn-to-turn fault is that while there may be high current in the fault itself, it is on a voltage base across the turns that are faulted. This can be illustrated by considering this case if the fault was between cables to two stationary contacts, or 1 1/4 percent of the total winding voltage of 7967 V. For a fault that meets the minimum O87P pickup of 0.3 pu, the differential current can be calculated based on the rated FLA of the transformer as well as the fault voltage, as shown in (10) and (11).

$$FLA = \frac{MVA \bullet 1{,}000}{\sqrt{3} \bullet kv} = \frac{84MVA \bullet 1{,}000}{\sqrt{3} \bullet 134.55kV} = 360.44A \quad (10)$$

$$I_{87P.min} = FLA \bullet 0.3 = 360.44\text{A} \bullet 0.3 = 108.13\text{A} \quad (11)$$

For a delta-wye-connected transformer, the turns ratio of the windings is the ratio of the high-side, line-to-line voltage to the low-side, line-to-neutral voltage, shown in (12)

$$n = \frac{V_{HS}}{\frac{V_{LS}}{\sqrt{3}}} = \frac{134.55\ kV}{\frac{13.8\ kV}{\sqrt{3}}} = 16.887 \quad (12)$$

An Ampere-turns (A-t) equivalent for this high-side current contribution can be calculated using the minimum 87P element pickup current and the turns ratio of the transformer in (13)

$$I_{87P.min} \bullet n = 108.13\ A \bullet 16.887\ turns = 1{,}826.08\ A - t \quad (13)$$

Balancing the Ampere-turns from the high side found in (13) and low side, we can calculate the low-side current needed to operate the 87P if a full low-side single-phase voltage were applied to the fault in (14).

$$\frac{1{,}826.08\ A - t}{1\ turn} = 1{,}826.08\ A \quad (14)$$

In comparison, the current for a turn-to-turn fault between two stationary contacts needed to pick up 87P is calculated as shown in (15).

$$\frac{1{,}826.08\ A - t}{1\frac{1}{4}\%\ turns} = 146.09\ kA \quad (15)$$

If the maximum stationary contact cable of the LTC is shorted to the nominal voltage cable, providing 10 percent of the voltage winding, the calculation would yield the fault current calculated in (16).

$$\frac{1{,}826.08\ A - t}{10\%\ turns} = 18.26\ kA \quad (16)$$

This requirement for an extremely high fault current to meet the minimum phase sensitivity illustrates the damage that may be caused by a turn-to-turn fault without an element like 87P being able to trip.

The 87Q element in comparison, has advantages that allow for better sensitivity. The first is that under normal load conditions, we expect to meter very little negative-sequence current. Because there is no load contribution to this element, it can inherently be designed to be more sensitive. The second is that while the 87P element looks at individual phases, the 87Q element takes the unbalance of all three phases for each winding into account. Because of this, a low-level fault in an individual phase shows up as unbalance when compared to unfaulted phases. The third is the design of the operate and restraint quantities themselves. For 87P elements, the operate current is typically the magnitude of the sums of the winding currents and restraint is the sum of the magnitude of the winding currents, which means the restraint gets a contribution from each terminal. For the 87Q element examined, the operate quantity is likewise the magnitude of the sum of the winding negative-sequence currents; however, the restraint is the maximum magnitude of the winding negative-sequence currents, meaning there is a lower overall contribution to the restraint, allowing for an inherently more sensitive element.

A comparison of sensitivity between the 87P and 87Q elements can be examined using an ideal single-phase fault on the low side of a delta-wye-connected transformer. A single-phase fault involving only C-phase of the wye winding will appear to be a B-C, phase-to-phase fault on the delta winding of the transformer.

An ideal B-C, phase-to-phase fault includes only positive and negative-sequence currents that are equal in magnitude and opposite in phase angle. Using a minimum pickup of 0.3 pu and examining an 87Q element that uses the magnitude of 3I2 as an operate quantity, we can calculate the sequence currents for this fault, shown in (17), (18), and (19).

$$I0 = 0\,pu \tag{17}$$

$$I1 = \frac{0.3 \angle 0^\circ}{3}\,pu = 0.1 \angle 0^\circ\,pu \tag{18}$$

$$I2 = \frac{0.3 \angle 180^\circ}{3}pu = 0.1 \angle 180^\circ\,pu \tag{18}$$

Using the definitions of symmetrical components, phase currents Ia, Ib, and Ic can also be calculated for this fault in (20), (21), (22), and (23).

$$\alpha = 1 \angle 120^\circ \tag{20}$$

$$Ia = I0 + I1 + I2 = 0\,pu + 0.1 \angle 0^\circ\,pu + 0.1 \angle 180^\circ\,pu = 0\,pu \tag{21}$$

$$Ib = I0 + I1 \bullet a^2 + I2 \bullet a = 0\,pu + 0.1 \angle 240^\circ\,pu + 0.1 \angle 300^\circ\,pu = 0.173 \angle 90^\circ\,pu \tag{22}$$

$$Ic = I0 + I1 \bullet a + I2 \bullet a^2 = 0\,pu + 0.1 \angle 120^\circ\,pu + 0.1 \angle 60^\circ = 0.173 \angle 90^\circ\,pu \tag{23}$$

Comparing the minimum negative-sequence current applied to this fault of 0.3 pu to the calculated phase currents of 0.173 pu, shows that the phase differential operate quantity is reduced by the square root of three compared to the contribution to the negative-sequence operate quantity for this particular case.

Examining the recorded data prior to the fault evolution that allowed the phase differential element of the in-service relay to trip, reveals that the 87Q element would have been picked up and had the potential to trip. These currents, while abnormal, were in a steady state at the beginning of the event recording. It can reasonably be concluded that this steady state was persistent for some time prior to this recording and that the 87Q element, had it been in service, would have been able to trip the transformer, clearing the fault prior to the evolution of the fault and additional damage caused before the 87P element asserted.

VI. Conclusion

Power transformers are a critical asset within the bulk electric system. As such, the protection of these key pieces of equipment requires careful consideration to ensure ample coverage while also allowing for the varying of system conditions throughout the lifecycle of the equipment. Phase differential protection is often relied upon as a key component of the primary and backup protection of transformers. Differential elements are touted for their speed and overall sensitivity. However, as we describe in this paper, partial windings faults can still be a challenge for traditional protection methods. Adding an additional layer of protection using a negative-sequence differential element allows for increased sensitivity for faults that have not evolved to the point where a phase differential element will operate. The early detection of an interturn fault can result in a lower severity in equipment damage as well as reduced downtime.

We estimate that by tripping earlier in the fault development (likely eliminating the need to drain and enter the main tank) the cost and time to repair the LTC mechanism would have been significantly reduced, potentially as much as 50 percent.

VII. Appendix A

Table I shows a complete list of the compensation matrices that are available in some modern microprocessor relays. A detailed description of the development and application of these matrices can be found in [3] and [4]. In Table I, *cw* indicates clockwise compensation, and *ccw* indicates counter-clockwise compensation.

TABLE I
COMPENSATION MATRICES

Matrix	Degrees Compensated		Calculation
0	ABC, 0 • 30° ccw	0°	$\begin{bmatrix}1&0&0\\0&1&0\\0&0&1\end{bmatrix}$
	ACB, 0 • 30°cw	0°	
1	ABC, 1 • 30° ccw	30°	$\frac{1}{\sqrt{3}}\begin{bmatrix}1&-1&0\\0&1&-1\\-1&0&1\end{bmatrix}$
	ACB, 1 • 30° cw	330°	
2	ABC, 2 • 30° ccw	60°	$\frac{1}{3}\begin{bmatrix}1&-2&1\\1&1&-2\\-2&1&1\end{bmatrix}$
	ACB, 2 • 30° cw	300°	
3	ABC, 3 • 30° ccw	90°	$\frac{1}{\sqrt{3}}\begin{bmatrix}0&-1&1\\1&0&-1\\-1&1&0\end{bmatrix}$
	ACB, 3 • 30° cw	270°	
4	ABC, 4 • 30° ccw	120°	$\frac{1}{3}\begin{bmatrix}-1&-1&2\\2&-1&-1\\-1&2&-1\end{bmatrix}$
	ACB, 4 • 30° cw	240°	
5	ABC, 5 • 30° ccw	150°	$\frac{1}{\sqrt{3}}\begin{bmatrix}-1&0&1\\1&-1&0\\0&1&-1\end{bmatrix}$
	ACB, 5 • 30° cw	210°	
6	ABC, 6 • 30° ccw	180°	$\frac{1}{3}\begin{bmatrix}-2&1&1\\1&-2&1\\1&1&-2\end{bmatrix}$
	ACB, 6 • 30° cw	180°	
7	ABC, 7 • 30° ccw	210°	$\frac{1}{\sqrt{3}}\begin{bmatrix}-1&1&0\\0&-1&1\\1&0&-1\end{bmatrix}$
	ACB, 7 • 30° cw	150°	
8	ABC, 8 • 30° ccw	240°	$\frac{1}{3}\begin{bmatrix}-1&2&-1\\-1&-1&2\\2&-1&-1\end{bmatrix}$
	ACB, 8 • 30° cw	120°	
9	ABC, 9 • 30° ccw	270°	$\frac{1}{\sqrt{3}}\begin{bmatrix}0&1&-1\\-1&0&1\\1&-1&0\end{bmatrix}$
	ACB, 9 • 30° cw	90°	
10	ABC, 10 • 30° ccw	300°	$\frac{1}{3}\begin{bmatrix}1&1&-2\\-2&1&1\\1&-2&1\end{bmatrix}$
	ACB, 10 • 30° cw	60°	
11	ABC, 11 • 30° ccw	330°	$\frac{1}{\sqrt{3}}\begin{bmatrix}1&0&-1\\-1&1&0\\0&-1&1\end{bmatrix}$
	ACB, 11 • 30° cw	300°	
12	ABC, 12 • 30° ccw	360°	$\frac{1}{3}\begin{bmatrix}2&-1&-1\\-1&2&-1\\-1&-1&2\end{bmatrix}$
	ACB, 12 • 30° cw	360°	

VIII. APPENDIX B

This appendix shows a summary of the relay settings for the device that were in service providing protection for the transformer during the event. These settings were used in the custom calculations created to investigate the performance of the 87Q element.

CT Ratio Winding 1: CTR1 (H Winding) = 80

CT Ratio Winding 2: CTR2 (X Winding) = 800

CT Ratio Winding 3: CTR3 (Y Winding) = 800

Max Transformer Power Capacity: MVA = 84.0

Internal CT Connection Compensation: ICOM = Y

Winding 1 CT Compensation: W1CTC = 0

Winding 2 CT Compensation: W2CTC = 1

Winding 3 CT Compensation: W3CTC = 1

Winding 1 Nominal Voltage: VWDG1 = 134.55 (no-load tap changer neutral position)

Winding 2 Nominal Voltage: VWDG2 = 13.8 (LTC neutral position)

Winding 3 Nominal Voltage: VWDG3 = 13.8 (LTC neutral position)

Winding 1 Current Tap: TAP1 = 4.51

Winding 2 Current Tap: TAP2 = 4.39

Winding 3 Current Tap: TAP3 = 4.39

Restrained 87 Element Pickup: O87P = 0.30

Restrained 87 Element Slope 1: SLP1 = 25 percent

Restrained 87 Element Slope 2: SLP2 = 60 percent

Restraint Slope 1 Limit: IRS1 = 3.0

Unrestrained 87 Element Pickup: U87P = 10

IX. APPENDIX C

This appendix shows the calculations that were used to examine the 87Q performance from within the event record that was recorded from the device in service.

I1W1C1 := IAW1.Phasor / TAP1.Set

I2W1C1 := IBW1.Phasor / TAP1.Set

I3W1C1 := ICW1.Phasor / TAP1.Set

3I2W1C1 := 3 • SEQ2(I1W1C1, I2W1C1, I3W1C1)

I1W2C1 := ((IAW2.Phasor / TAP2.Set) – (IBW2.Phasor / TAP2.Set))/sqrt(3)

I2W2C1 := ((IBW2.Phasor / TAP2.Set) – (ICW2.Phasor / TAP2.Set))/sqrt(3)

I3W2C1 := ((ICW2.Phasor / TAP2.Set) – (IAW2.Phasor / TAP2.Set))/sqrt(3)

3I2W2C1 := 3 • SEQ2(I1W2C1, I2W2C1, I3W2C1)

I1W3C1 := ((IAW3.Phasor / TAP3.Set) – (IBW3.Phasor / TAP3.Set))/sqrt(3)

I2W3C1 := ((IBW3.Phasor / TAP3.Set) – (ICW3.Phasor / TAP3.Set))/sqrt(3)

I3W3C1 := ((ICW3.Phasor / TAP3.Set) – (IAW3.Phasor / TAP3.Set))/sqrt(3)

3I2W3C1 := 3 • SEQ2(I1W3C1, I2W3C1, I3W3C1)

IOP87Q := MAG(3I2W1C1 + 3I2W2C1 + 3I2W3C1)

IRT87Q := MAX(MAG(3I2W1C1), MAX(MAG(3I2W2C1), MAG(3I2W3C1)))

87QP := 0.3

SLPQ := 0.25

SLPQ.calc := IOP87Q / IRT87Q

87QPout := IOP87Q > 87QP AND SLPQ.calc > SLPQ

X. REFERENCES

[1] M. J. Thompson, “Percentage Restrained Differential, Percentage of What?” proceedings of the 37th Annual Western Protective Relay Conference, Spokane, WA, October 2010.

[2] B. Kasztenny, M. Thompson, and N. Fischer, “Fundamentals of Short Circuit Protection for Transformers,” proceedings of the 63rd Annual Conference for Protective Relay Engineers, College Station, TX, March 2010.

[3] B. Edwards, D. G. Williams, A. Hargrave, M. Watkins, and V. K. Yedidi, “Beyond the nameplate - Selecting Transformer Compensation settings for Secure Differential Protection,” 2017 70th Annual Conference for Protective Relay Engineers (CPRE), College Station, TX, 2017, pp. 1-23.

[4] A. Hargrave, J. Hostetler, and M. Thompson, "Beyond the Nameplate: Transformer Compensation Revisited – New Applications, Greater Simplicity," in 76th Annual Georgia Tech Protective Relaying Conference, Atlanta, GA, USA, May 3–5, 2023. Available: https://selinc.com/api/download/138123/

[5] B. Kasztenny, N. Fischer, and H. J. Altuve, "Negative-sequence differential protection – principles, sensitivity, and security," 2015 68th Annual Conference for Protective Relay Engineers, College Station, TX, 2015, pp. 364–378.

[6] J. Mraz, J. Pomeranz, and J. Law, "Limits of Sensitivity for Detecting Inter-Turn Faults in an Energized Power Transformer," proceedings of the 34th Annual Western Protective Relay Conference, Spokane, WA, October 2007.

[7] IEEE Standard C57.12.00-2021, *IEEE Standard for General Requirements for Liquid-Immersed Distribution, Power, and Regulating Transformers.*

XI. Biographies

Craig Cosgrove is an electrician at MATEP LLC., a tri-generation facility providing energy to The Longwood Medical Area of Boston, and has been working in protection and control for 18 years.

Austin Burfield received a Bachelor of Science in Electrical and Computer Engineering from The Ohio State University in 2011, and a Master of Engineering from the University of Cincinnati in 2025. Upon graduation from undergrad, he transitioned to full time at SEL as an Application Engineer specializing in protection. In 2018, Austin joined the Transmission Engineering group of Duke Energy as a P&C Engineer. In 2022 Austin returned to SEL where he is currently a Senior Application Engineer. Austin is a registered Professional Engineer in the State of Ohio and is a Senior Member of IEEE.

Zachary Summerford earned his BS in electrical and computer engineering with a focus on power systems and digital logic design from The Ohio State University in 2012. He earned his ME in electrical engineering with a focus on power systems from the University of Idaho in 2022. He began working for Schweitzer Engineering Laboratories, Inc. (SEL) in 2012 and served as a senior application engineer for protection until 2024. He is currently a lead sales engineer for SEL. He is a senior member of IEEE and a registered Professional Engineer (PE) in Ohio.